Al-Azhar Bulletin of Science

Volume 28 | Issue 1 Article 12

6-1-2017
Section: Chemistry

REMOVAL OF SOME TOXIC IONS FROM INDUSTRIAL WASTEWATER USING BATCH TECHNIQUE BY INDION 225NA RESIN

A. Swelam
Chemistry Department, Faculty of Science, Al-Azhar University, Cairo, Egypt.

M.B. Awad
Chemistry Department, Faculty of Science, Al-Azhar University, Cairo, Egypt.

M. Saber
Chemistry Department, Faculty of Science, Al-Azhar University, Cairo, Egypt.

Follow this and additional works at: https://absb.researchcommons.org/journal

 Part of the Life Sciences Commons

How to Cite This Article

Swelam, A.; Awad, M.B.; and Saber, M. (2017) "REMOVAL OF SOME TOXIC IONS FROM INDUSTRIAL WASTEWATER USING BATCH TECHNIQUE BY INDION 225NA RESIN," *Al-Azhar Bulletin of Science*: Vol. 28: Iss. 1, Article 12.
DOI: https://doi.org/10.21608/absb.2017.8116

This Original Article is brought to you for free and open access by Al-Azhar Bulletin of Science. It has been accepted for inclusion in Al-Azhar Bulletin of Science by an authorized editor of Al-Azhar Bulletin of Science. For more information, please contact kh_Mekheimer@azhar.edu.eg.

REMOVAL OF SOME TOXIC IONS FROM INDUSTRIAL WASTEWATER USING BATCH TECHNIQUE BY INDION 225NA RESIN

A.A. Swelam, M.B. Awad and M.Saber

Chemistry Department, Faculty of Science, Al-Azhar University, Cairo, *Egypt.*

ABSTRACT

In this study, the adsorptive capacity of the synthetic Indion 225Na cation exchange resin was evaluated for the removal of different ions species from Oil Refining Company wastewater. Batch studies were performed to evaluate the effects of various experimental parameters by such as pH, contact time, temperature, resin and initial concentrations on the removal ion species. The Indion resin was characterized using FT-IR spectroscopy and scanning electron microscopy were used to analyse the resin. The adsorption kinetics were fitted by the pseudo-first-order, pseudo-second-order kinetic equations and intra-particle diffusion model. The thermodynamic parameters, sticking probability and activation energy of the removal processes were also evaluated. Based on these results, the synthetic Indion 225Na resin could be applied for treatment of industrial effluents which are rich in inorganic pollutants.

1. INTRODUCTION

The pollution of water by metal ions has attracted increasing major attention due to their importance in industrial processes and their potential toxicity towards humans and in the aquatic environment. All crude oils, especially petroleum samples contain several inorganic components. Several metal ions traces have found by one of two forms in the petroleum oils. Either as an organometallic porphyrin related to the organic material or as a non-porphyrin metal which existe in the resin or asphaltic fraction of the oil [1]. Thus, ion exchange technique is a mature, well which easy to regenerate beneficial effect, for treating hazardous effluent and recovery this contamination. Ion exchange technique is highly effective with low-cost materials, efficient, as well as easy to operate among physicochemical treatment processes [2]. Mesoporous silica is similar to the adsorption process by which was demonstrated by researchers [3] and graphene oxide [4]. Recently, ion exchange technology has been applied to treat various pollutants from wastewater [5].

The aim of this work is to develop a batch process for the removal of different ions already presented in the Oil Refining Company and recovering the valuable ions by regeneration of ion exchange resin. The resin adsorption kinetics and thermodynamic parameters were evaluated and discussed for Indion 225Na resin. To ensure its applicability to the industrial ions in wastewater, we have to study the effects of pH, resin dose, temperature and ion initial concentration.

2. EXPERIMENTAL

2.1. Chemicals

All chemicals/reagents used in this study were purchased from Sigma-Aldrich and Fisher scientific. All chemicals were used without further purification. The Indion 225Na resin was provided by ion exchange (India) Limited. Before use, the Indion resin was washed by distilled water to clean the surface and then dried at 60 °C. After drying, the resin was used for adsorption study.

2.2. Characterization studies

Fourier Transforms Infrared Spectrometer (FTIR), Mobile IR - Portable FT-IR, Manufacturer by Bruker Optik GmbH was used. The FTIR spectra (400 - 4000 cm^{-1}) measured at room temperature was used to investigate any observed changes of the synthetic resin with Indion 225Na, and these included new peaks, intensity variations of

peaks originally present and wavelength shifts. A Scanning Electron Microscope (SEM) with Energy-Dispersive X-ray Spectrometer (EDX), High-vacuum 200V – 30Kv up to 2µA – continuously adjustable 3.0nm at 30kV (SE) 10nm at 3kV (SE) 4.0nm at 30kV (BSE) Low-vacuum 3.0nm at 30kV (SE) 4.0nm at 30kV (BSE) < 12nm at 3kV (SE) was used to obtain an image of the resin before and after loading of metal hydroxides. EDX detector which was attached to the SEM system was used to investigate the distribution of ions lines of the prepared resins before and after adsorption. Agilent technology model 7700 series ICP- MS its provide unparalleled accuracy in high-matrix samples, redefining cell performance in helium mode with a revolutionary 3rd generation cell design made in Germany. The Dionex ICS-3000 Ion Chromatography. Dionex Corporation is an American Company. WTW Thermoreactor CR 3200 for COD Germany. Analytik Jena Multi N/C 2100 S TOC TNb Total Organic Carbon Analyzer (TOC) Germany

2.3. Wastewater samples

The wastewater samples were used to evaluate the removal efficiency of the Indion resin for the pollutant ions. The wastewater samples were collected from oil refining Company Mostorod, Kaliobeya Governorate. All the samples solutions were homogeneously mixed using a Magnetic stirrer provided with heating a hot plate (models MSH) for 3 h. The data of the wastewater analysisare listed in Table 1.

Table 1. Analysis of wastewater samples.

Date of collection	January 2017
pH	6.76
TDS	1845 ppm
Specific Conductivity	3430 µS/cm
COD	24 ppm
BOD	40 ppm
TOC	9 ppm
ICP results	Ag(7.65), Pb(0.691), Ba(216.99), Ni(842) Na(2000), Fe(0.065), Mo(19.79), Ca(71.07), Mn(144.22), Mg(19), K(10.1), Cu(38.85), Co(0.851), Al(41.09), Cd(20.52), Cr(6.44), V(4.05), Zn(22.29), As(2.87), Se(19.67) and Sb(3.04) ppm
Ic results	F(1.466), Cl(871.41), NO_2(-), Br(5.46.16), NO_3(24.7678) and SO_4(82.5627) ppm

2.4. Adsorption procedure

The optimization of adsorption parameters was performed by mixing 0.25 g of the Indion resin with 25 mL solutions containing a mixture of metal and nonmetal ions at 24 ^{0}C and which agitated at 100 rpm in the shaker at different time intervals. After a certain time intervals, the concentration of the ions in the supernatant was measured using AAS. The adsorbate amount at equilibrium can be evaluated by relationship:

$$q_e = \frac{(C_o - C_e)V}{W \times 1000} \quad \text{----------} \quad (1)$$

and the removal percentage yield (R %) was calculated as follows:

$$(R\ \%) = \frac{C_o - C_e}{C_o} \times 100 \quad \text{----------} \quad (2)$$

where C_0 and C_e are the initial and the equilibrium concentrations of the ion (mg/l), respectively, V is the volume of the solution (ml), and W is the mass of adsorbent (g). All the experiments were run three times, and the reported values represent the averages.

3. RESULTS AND DISCUSSION

3.1. Characterization studies

Scanning electron microscope (SEM) imaging was used to investigate the morphology of the Indion 225Na resin.

Representative images of the resin before and after ions-loaded are shown in Figs. 1 and 2, respectively. The particle size of the Indion resin used is within the range 265.20–1691.13 µm while the average particle size is 449.99. µm. The surface morphology of the Indion resin before its loading by the regarded ions where SEM-EDX spectrum revealed the presence of the elements C, O, S and Na. Fig.1 shows spherical particles of smooth surface. which is a characteristic feature smooth expansion, when it is subjected to expanded bed adsorption. Fig. 2 shows a change of the surface morphology of the resin after its loading by some ions into the wastewater where SEM-EDX confirmed the presence of elements (Co, K, As and Ca) in the loaded resin that, some ions were adsorbed onto the surface of the resin.

FTIR spectra of Indion ion-exchange resin before and after the adsorption process are presented in Fig.3A and, B. The absorption bands at ~ 2925, 1495, 1035 and 670 cm^{-1} are aroused due to the symmetric and asymmetric vibrations of C-H, C-C, S-O and C-S existed in Indion resin [6]. Band at 1411 cm^{-1} is due to SO_3^- asymmetric and sharp peaks at 1007 and 1035/cm is due to SO_3 symmetric stretching. The peaks at 1411–1634 cm^{-1} are due to deformation and skeletal vibrations of C-H bond in divinylbenzene. Two significant changes are observed in FTIR spectrum of the Indion resin after the adsorption of the ions from wastewater. The peak at 2110 cm^{-1} is disappeared after the adsorption process and new peaks appear at 1638 cm^{-1}, 1525 cm^{-1} and 1635 cm^{-1} due to the C=O group vibrations [7]. The absorption band at 1125 cm^{-1} in FTIR spectrum of Indion ion-exchange resin is also shifted to 1122 cm^{-1} because of the high electron density which is induced via an electrostatic interaction after adsorption of the ions from the wastewater. However the other functional groups remained intact during the adsorption process [7,8].

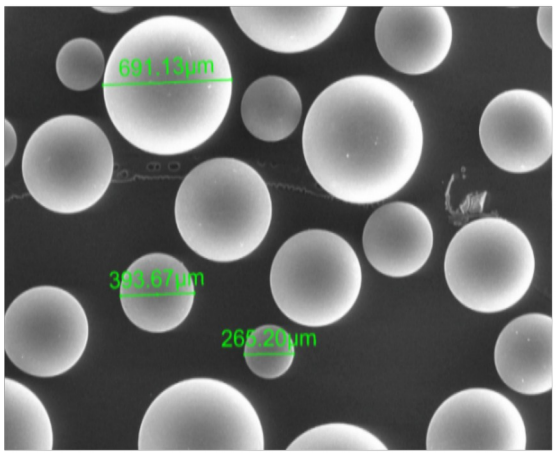

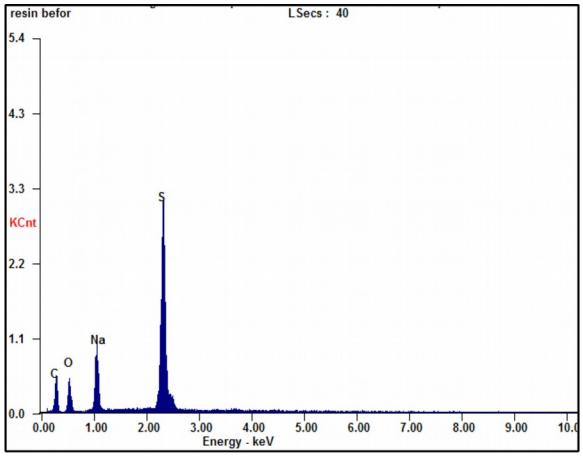

Element	C K	O K	Na K	S K
Wt %	52.48	17.37	10.45	19.71
At %	66.97	16.64	06.97	09.42

Fig. 1. SEM and EDX spectra of the Indion resin before ions-loaded.

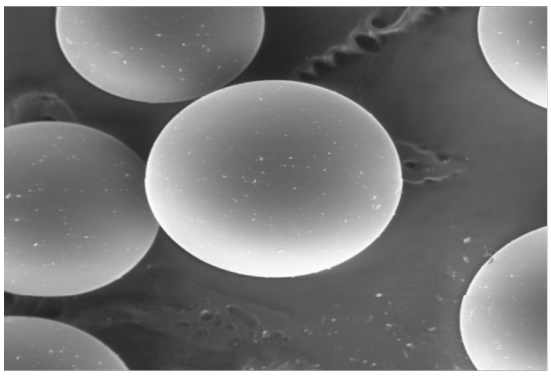

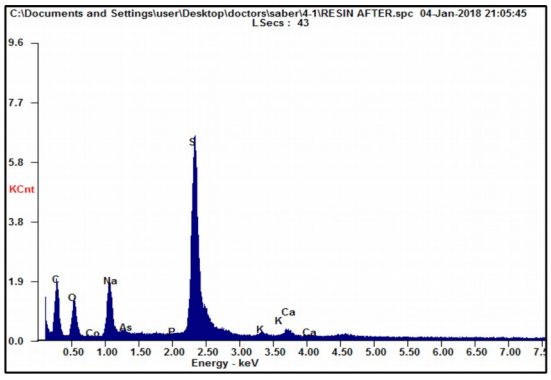

Element	C K	O K	Co L	Na K	As L	P K	S K	K K	Ca K
Wt %	59.24	17.84	00.40	07.39	01.11	00.06	13.10	00.25	00.61
At %	72.30	16.34	00.10	04.71	00.22	00.03	05.99	00.09	00.22

Fig. 2. SEM and EDX spectra of the Indion 225Na resin after ions-loaded.

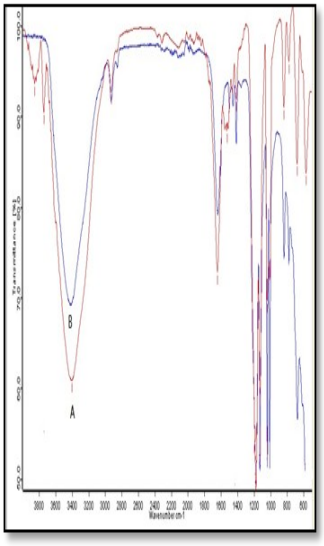

Fig.3. FTIR spectra of the Indion ion-exchange resin (A) before and (B) after the adsorption process

3.2. Effect of the resin dose

The dosage effect of the Indion 225Na resin on the percentage of metal and nonmetal ions removed from wastewater was studied using ion concentrations of the mother raw solution (ppm) (Table 2) which revealed that the removal efficiencies of the metal ions increased gradually with increasing amounts of the resin and this increase in % adsorption may be attributed to the fact that the more adsorbent dose the greater surface area or the more is adsorption sites for the ions [9].

3.3. Effect of competition

Water contaminated are frequently more than just one metal and nonmetal ion, as co-exist ions and compete for binding to different ligands in the environment. Hence we have to study the competitive adsorption of the different ions which indeed exist in the wastewater of the petroleum factory onto the Indion resin. Although the ions under study are of different valences, each of them interacts with the surface functional groups of the resin in different ways with different capacities.

Table 2. Effect of the resin dosage (g) on removal percentage(%)

Ion	0.125g	0.25g	0.5g	1.0g	1.5g
Ag	13.725	15.163	47.712	73.856	98.693
K	10.891	16.733	77.030	86.733	89.307
Ba	90.783	92.871	95.852	98.617	99.493
Co	4.465	52.174	57.697	40.306	40.31
Zn	10.767	81.247	89.726	91.162	91.341
Cd	41.520	72.027	75.585	90.156	95.078
Pb	59.479	68.162	73.372	68.307	64.834
Ca	90.151	90.910	97.186	98.452	99.887
Mg	86.842	88.895	99.137	99.205	99.616
Mn	96.672	96.755	97.927	98.662	99.356
Cu	40.952	41.184	59.022	62.960	63.681
Ni	100.00	100.00	98.931	83.373	80.998
Mo	84.336	84.942	92.623	93.178	94.290
Al	51.326	51.910	73.229	82.648	99.457
Cr	15.217	24.224	49.689	59.161	67.547
Fe	70.770	70.770	75.390	81.540	46.150
V	11.111	37.778	79.210	81.432	83.506
As	12.195	39.373	44.251	49.129	59.233
Sb	44.079	46.711	60.526	70.395	34.211
Se	28.826	30.300	40.163	45.196	28.114

The results obtained in this work using Indion 225Na-form with the Sulphonic acid functional groups indicated that. The selectivity % of the resin for the different ions follows the order: Ni(II) > Mn(II) > Ba(II) > Ca(II) > Mg(II) > Mo(II) > Zn(II) > Cd(II) > Fe(III) > Pb(II) > Co(II) > Al(III) > Sb(III) > Cu(II) > As(III) > V(III) > Se(III) > Cr(III) > K(I) > Ag(I). Moreover, the selectivity of the resin can be also analysed via structural characteristics of metal ions: the electrical load (charge), crystallographic ionic radii, van der Waals or covalent radii, ionization energy and electronegativity on Pauling scale, as well as the characteristics of functional groups of the resin, on the other hand [10].

There is a poor understanding of the order of binding of the ions by solid adsorbents like Indion cation exchange resin. Stafiej and Pyrzynska [11] studied the adsorption characteristics of certain divalent metal ions (*i.e.*,Cu, Co, Cd, Zn, Mn, and Pb) by MWCNTs and found that the affinity of metal ions for MWCNTs followed the order Cu(II) > Pb(II) > Co(II) > Zn(II) > Mn(II). Meanwhile, Li et al. [12] studied the competitive adsorption of Pb(II), Cu(II) and Cd(II) ions by oxidized MWCNTs and found that the adsorption capacities of MWCNTs for the three metal ions were in the order Pb(II) > Cu(II) > Cd(II). In the present study, it was observed that binding to both MWCNTs followed the order Cu(II) > Pb(II) ≈ Zn(II) > Cd(II) for % adsorption.

Unfortunately, there is no consensus in the competitive adsorption of the ions, as researchers have attributed their different affinities to different factors. These factors are related to the properties of these ions in aqueous solution and could affect surface binding and interaction energies or the accessibility of surface centers, which can be linked to the size of the species adsorbed. Although Pb(II) and Cd(II) have the largest radii (1.33 Å and 0.97 Å, respectively), they show lower adsorption than Zn(II), which have smaller ionic radii (0.72 Å). Thus, the smaller the ionic radius, the easier it is for a metal ion to penetrate through the boundary layer and adsorb onto the resin surface. Electronegativity (Pauling) is listed in the following order: Pb(II) > Cu(II) > Cd(II) > Zn(II) (*i.e.*, 2.33, 1.90, 1.69, and 1.65, respectively). This order does not agree well with the experimental affinities for binding and adsorption by the resin. The high adsorption and binding of Cu(II) to the resin compared with other ions (As(III), V(III), Se(III), Cr(III), K(I) and Ag(I)) can be explained. Because Cu(II) is predominantly specifically adsorbed (inner-sphere complexation), increasing the amount of more strongly bonded Cu is expected to reduce the number of sites available for other ions adsorption. Furthermore, Cu(II) is stabilized by the Jahn–Teller effect. The d^9 electronic configuration of this ion provides three electrons with two degenerate e_g orbitals and six electrons to the t_{2g}, leading to a doubly degenerate electronic ground state and a large energetic stabilization. A similar effect was observed in a multi-component system, where an increase in the Cu concentration resulted in a reduction of the uptake of other heavy metals [13]. Additionally, it was reported that high copper adsorption was caused by its ability to be reduced by the resin surface. Therefore, Cu(II) ions in close proximity to the resin surfaces are reduced after being attracted to cation exchange centers on the resin surfaces. The copper ions then vacate the cation exchange site for the adsorption of other ions [14]. Conversely, the lower adsorption of Ag(I) might be due to its lower tendency to form hydrolysis products and the fact that its ions do not compete effectively for variable charge surfaces, such as Indion resin. As a result, its adsorption is restricted to permanently charged sites [15].

3.4. Kinetic modeling

In order to investigate the mechanism and to determine the rate controlling step of adsorption of pollutants species on the Indion resin, kinetic models were used. The rate constants were calculated by using pseudo-first-order and pseudo-second-order kinetic models while the rate controlling step was determined by intra-particle diffusion model.

Pseudo-first-order model

Pseudo-first-order model generally expressed as follows [16]:

$$\frac{dq}{dt} = k_1(q_e - q_t) \text{ ---------- (3)}$$

where q_e and q_t are the amount of metal sorbed per unit weight of the sorbent at equilibrium and at any time t, respectively (mg/g) and k_1 is the rate constant of pseudo-first order sorption (min^{-1}). After integration and applying boundary conditions, for $t = 0$, $q = 0$, the integrated form of Eq. (3) becomes

$$\ln(q_e - q_t) = \ln q_{e,1} - k_1 t \text{ ---------- (4)}$$

The values of rate constant (k_1) and equilibrium capacity ($q_{e,1,cal}$) can be obtained from the slope and intercept, respectively by plotting log ($q_e - q_t$) against time 24^{0}C, 35^{0}C and 50^{0}C.

Pseudo-second-order rate model

Pseudo-second-order rate model [17] is given as follows:

$$\frac{dq}{dt} = k_2(q_e - q_t)^2 \text{ ---------- (5)}$$

where k_2 is the rate constant of pseudo-second order sorption $(\text{gm mmol}^{-1}\ \text{min}^{-1})$, q_e is the amount of sorbate at equilibrium (mg/g) and q_t is the amount of sorbate on the surface of the resin surface at any time t (mg/g).

Integrating this equation (5) for the boundary conditions for $t = 0,\ q = 0$ gives

$$\frac{t}{q} = \frac{1}{k_2 q_{e,2}^2} + \frac{1}{q_{e,2}} t \quad \text{---------} \quad (6)$$

The values of k_2 can be determined from the plot of t/q versus t, furthermore, the initial rate of adsorption (h) (mg/g min), when $t \rightarrow 0$, can also be calculated by using following formula:

$$h = k_2 q_{e,2}^2 \quad \text{----------} \quad (7)$$

Table 3 provides the pseudo-first-order rate constant k_1 and pseudo-second-order rate constant k_2, calculated equilibrium adsorption capacity $q_{e\ (cal)}$ and experimental equilibrium adsorption capacity $q_{e\ (exp)}$ for all the ions at different initial metal ion concentrations (mg/L). The $q_{e(cal)}$ values of the pseudo-first-order kinetic model disagree with those of experimental $q_{e\ (exp)}$. However, for the pseudo-second-order kinetic model the calculated $q_{e(cal)}$ agree well with $q_{e(expl)}$ for all the ions. Further, the values of correlation coefficients (R^2) of pseudo-first-order model were slightly lower than those of pseudo-second-order model indicating that the pseudo-second-order model [18] well fitted than pseudo-first-order model. The initial adsorption rate (h) for Ag, Co, Cu, Zn, Al, Sb, Se and V ionic species were 0.0645, 0.0015, 0.0986, 0.1693, 0.2026, 746.2687, 0.0462 and 0.0081 mg/g min, respectively, indicating the highest adsorption rate of these ions on to the Indion resin. On the other hand, the correlation coefficients (R^2) values of pseudo-first-order model were higher than pseudo-second-order model indicating that the pseudo-first-order model is well fitted than pseudo-second-order model (K, Ba, Ca, Cd, Co, Mg, Mn, Pb, As, Cr, Fe, Mo and Se species).

Intra-particle diffusion model (Waber–Morris model)

The overall reaction for the adsorption of the different ions is a pseudo-second-order and pseudo- first order reactions. However, this could not kinetically follows on the rate-limiting step. The rate-limiting step may be either the boundary layer (external film) or the intra-particle (pore) diffusion of ion on the Indion resin surface from bulk of the solution in a batch process. The probability of the intra-particle diffusion was explored using Weber and Morries equation [19].

$$q_t = K_i\, t^{0.5} + C \quad \text{----------} \quad (8)$$

where q_t is adsorption capacity at any time t and k_i is the intra-particle diffusion rate constant (mg/g $min^{½}$) and C (mg/g) is the film thickness. Greater the value of C greater is the effect of boundary layer on adsorption process. If the rate limiting step be the intra-particle diffusion, the plot of q_t against the $t^{1/2}$ should be a straight line and pass through the origin. The deviation of the plot from the linearity indicates the rate-limiting step should be boundary layer (film) diffusion controlled [9]. The intra-particle diffusion model parameters for adsorption of the ion species onto the resin at 24, 35 and 50 ^{0}C were calculated and listed in Table 3.

3.5. Effect of temperature

To study the effect of temperature parameter on the uptake of the ion species by the resin, temperatures of 24, 35 and 50 °C were selected. Hence, the uptake % of the various ions by the Indion resin are reported in Table 4 indicates that the adsorption of ion species on the Indion resin is endothermic [20]. Besides, the removal of Ni(II) by the Indion resin did not change significantly due to adsorption attained 100%.

3.6. Thermodynamic parameters

The thermodynamic parameters of the various ions presented in the wastewater were calculated at 24^{0}C, 35^{0}C and 50^{0}C are presented in Tables 5a and b.

The obtained sorption data were used to calculate the thermodynamic parameters.

Table 3-The kinetic parameters for adsorption of the ion species.

Ion	Pseudo-first order			Pseudo-second order				Intraparticle diffusion		
	$q_{e,1,cal}$	k_1	R^2	$q_{e,2,cal}$	k_2	h	R^2	K_i	C	R^2
Ag	0.0124	0.014	0.934	0.1169	4.7207	0.0645	0.999	0.001	0.101	0.952
K	0.19	0.040	0.980	0.3068	0.0412	0.0039	0.480	0.020	0.01	0.810
Na	9.429	0.017	0.913	144.3001	0.0074	155.0388	1.000	1.047	132.361	0.975
Ba	26.72	0.038	0.960	55.7724	0.0001	0.3052	0.137	2.363	3.731	0.896
Ca	5.357	0.056	0.858	15.8781	0.0005	0.1211	0.127	0.599	1.049	0.502
Cd	1.924	0.032	0.973	-0.8671	0.0078	0.0058	0.020	0.183	0.399	0.917
Co	0.050	0.040	0.920	0.0598	0.4251	0.0015	0.920	0.040	0.020	0.910
Cu	1.200	0.040	0.850	1.8957	0.0274	0.0986	0.960	0.140	0.310	0.660
Mg	1.410	0.050	0.870	0.6315	0.0131	0.0052	0.130	0.160	0.220	0.520
Mn	16.04	0.050	1.000	19.0767	0.0014	0.5228	0.900	1.390	0.650	0.800
Pb	0.050	0.020	0.850	0.5734	0.0013	0.0004	0.320	0.010	0.010	0.890
Zn	1.130	0.030	0.930	1.9626	0.0440	0.1693	1.000	4149	12.54	0.510
Al	2.1360	0.066	0.759	2.3832	0.0357	0.2026	0.993	0.169	0.568	0.689
As	1.193	0.031	0.975	3.0376	0.0016	0.0152	0.199	0.118	0.173	0.913
Cr	0.150	0.020	0.990	0.2512	0.0567	0.0036	0.940	0.020	0.010	0.980
Fe	19.62	0.020	0.970	19.8768	0.0002	0.0909	0.120	2.080	5.430	0.980
Mo	2.170	0.040	0.980	11.1099	0.0002	0.0198	0.240	0.200	0.350	0.910
Sb	0.130	0.030	0.990	30.2480	0.8156	746.2687	1.000	0.010	30.11	0.910
Se	0.530	0.050	0.990	0.6777	0.1005	0.0462	0.990	0.050	0.130	0.760
V	79.86	0.310	0.780	0.1804	0.2497	0.0081	0.990	0.010	0.020	0.940

Table 4. Effect of the solution temperature on the uptake % of various ions

Ion	24^{0}C	35^{0}C	50^{0}C		Ion	24^{0}C	35^{0}C	50^{0}C
Ag	15.16	15.56	35.45		Cu	41.18	45.56	48.21
K	16.73	20.20	36.63		Ni	100.0	100.0	100.0
Ba	92.87	99.24	99.18		Mo	84.94	91.11	94.49
Co	52.17	62.52	73.44		Al	51.91	80.53	87.83
Zn	81.25	85.87	95.29		Cr	24.22	26.71	40.37
Cd	72.03	85.33	93.81		Fe	70.77	73.85	76.92
Pb	68.16	78.29	83.50		V	37.78	49.38	58.03
Ca	90.91	93.44	92.71		As	39.37	47.74	61.32
Mg	88.90	91.47	90.53		Sb	46.71	54.61	63.82
Mn	96.76	97.55	99.14		Se	30.30	86.48	96.04

The Gibbs free energy change, ΔG (kJ/mol) was calculated from the following equation;

$$\Delta G^{o} = \Delta H^{o} - T\Delta S^{o} \quad \text{----------} \quad (9)$$

The van't Hoff isochore equation [10]:

$$\ln K_C = \frac{\Delta S^{o}}{R} - \frac{\Delta H^{o}}{RT} \quad \text{----------} \quad (10)$$

The values of ΔH and ΔS were obtained from the slope $\left(\frac{-\Delta H}{R}\right)$ and intercept $\left(\frac{\Delta S}{R}\right)$, respectively, of the plot of $\ln K_c$ vs. $\frac{1}{T}$.

Equilibrium constant (K_c) was calculated using the following equation:

$$K_C = C_1/C_2 \quad \text{----------} \quad (11)$$

where C_1 (mg/l) is the amount of the metal ions adsorbed per unit mass of the magnetic ferric oxide nanoparticles and C_2 (mg/l) is the concentration of the metal ions in aqueous phase.

The negative values of ΔG^0 of Ag, Ba, Ca, Mn, Pb, Mn, Zn, Fe, Mo and Sb, indicate that the adsorption is thermodynamically feasible and spontaneous with great preference of ions for the resin surface of at 24^{0}C, 35^{0}C and 50^{0}C studied herein whereas the ΔG^0 values of Cd, As and Se species were positive at 24 and 35 ^{0}C while the negative value was observed at 50 ^{0}C. An opposite trend was observed for K, Co, Cu, Al, Cr, and V species where non-spontaneous nature of adsorption process of these ions is detected. The positive values of ΔH^0 indicate that the adsorption process is endothermic and the binding between the ionic species and the Indion resin is strong. Moreover, the magnitude of ΔH^0 can provide information about adsorption which belongs to physisosorption (2.1–20.9 kJ/mol) or chemisorption (80–200 kJ/Mol) [22].. ΔS^0 is a measure of randomness in the system. The positive value indicates that affinity of Ag, K Ba, Ca, Cd, Co, Cu, Mg, Mn, Pb, Al, Cr, Fe, Mo, V, As, Sb and Se for the sorption sites is high, and randomness at the solid/solution interface increases during the adsorption process. The negative values of ΔS^0 reflect the reduction of randomness of the adsorption system. For Zn sorption on the Indion 225Na resin the value of ΔS^0 is equals to -0.1043 and corresponds to a decrease in a freedom degree of the adsorbed species.

In order to further support the assertion that the adsorption is the predominant mechanism, the values of the activation energy (E_a) and sticking probability (S*) were estimated from the experimental data. They were calculated using a modified Arrhenius type equation **[23]** related to surface coverage as expressed in equations (12,13):

$$\theta = 1 - \frac{C_e}{C_o} \quad \text{----------} \quad (12)$$

$$S^{*} = (1-\theta)\exp\left(-\frac{E_a}{RT}\right) \quad \text{---------} \quad (13)$$

The apparent activation energy (E_a) and the sticking probability (S*) are estimated from the plot (Fig. not shown). The sticking probability, S*, is a function of the adsorbate/adsorbent system under consideration and depends on the temperature of the system. The parameter S* indicates the measure of the potential of an adsorbate to remain on the adsorbent indefinitely cited in Table 5a and b. The effect of temperature on the sticking probability was evaluated at 24^{0}C, 35^{0}C and 50^{0}c by calculating the surface coverage. Table 5a and b, also indicated that the values of S* ≤ 1. Hence the sticking probability of the Ag, K, Ca, Co,Cu, Mg, Pb, As, Cr, Fe, Sb and V onto the adsorbent system is very high. While the

sticking probability of the Ba, Cd, Mn, Zn, Al, Mo and Se species was > 1. This means that the adsorbent system is low. According to Arrhenius equation, activation energy of the adsorption KJ/Mol) can be calculated using the above equation (13). The magnitude of activation energy gives an idea about the type of adsorption which is mainly physical or chemical. Low activation energies (<40 kJ mol^{-1}) are characteristics for physical adsorption, while higher activation energies (>40 kJ mol^{-1}) suggest chemical adsorption [24].

The calculated Ea for the adsorption of Ba, Cd, Al and Se ions on to the Indion 225Na resin values, indicate the chemical adsorption process of these adsorbates on the Indion resin. The positive value of the apparent activation energy E_a also indicates that the lower solution temperature favours the adsorption process. Whereas, the calculated Ea values (KJ/Mol) for the adsorption of Ag, K, Ca, Co, Cu, Mg,Mn, Pb, Zn, Al, As, Cr, Fe, Mo, Sb, Se and V ions on the adsorbent sample kJ/mol, indicated the physical adsorption process of these adsorbates on the Indion resin.

Table 5a- Thrmodynamic parameters for adsorption of the metal ions (petroleum Factory.

Ions	T ^{0}C	ΔG^0	ΔH^0	ΔS^0	R^2	S*	Ea	R^2
Ag	**24^{0}C** **35^{0}C** **50^{0}C**	-0.0399 -0.0751 -0.1232	0.9118	0.0032	**0.167**	**0.056896583**	**6.7031**	**0.71**
K	**24^{0}C** **35^{0}C** **50^{0}C**	9.6393 9.0159 8.1658	26.472	0.0567	**0.53**	**0.054495345**	**6.7403**	**0.42**
Na	**24^{0}C** **35^{0}C** **50^{0}C**	3.3647 3.4583 3.586	0.8366	-0.0085	**0.96448**	**0.219990701**	**0.6036**	**0.96382**
Ba	**24^{0}C** **35^{0}C** **50^{0}C**	1.7355- 4.2655- -7.7155	66.5739	0.23	0.571	2.01E-13	64.619	**0.75052**
Ca	**24^{0}C** **35^{0}C** **50^{0}C**	-0.1795 -0.4756 -0.8793	7.8143	0.0269	**0.26131**	**0.004632**	**7.185**	**0.255**
Cd	**24^{0}C** **35^{0}C** **50^{0}C**	3.0842 1.4596 -0.7558	46.9487	0.1477	**0.89**	**2.73E-08**	**39.665**	**0.8544**
Co	**24^{0}C** **35^{0}C** **50^{0}C**	5.3331 4.6189 3.645	24.6169	0.0649	**0.89**	**0.000901**	**15.421**	**0.84**
Cu	**24^{0}C** **35^{0}C** **50^{0}C**	6.4951 6.4459 6.3788	7.8234	0.0045	**1**	**0.141859**	**3.4815**	**0.99**
Mg	**24^{0}C** **35^{0}C** **50^{0}C**	0.3988 0.1933 -0.0868	5.9458	0.0187	**0.1**	**0.01207**	**5.3439**	**0.09**
Mn	**24^{0}C** **35^{0}C** **50^{0}C**	-6.927 -14.92 -25.83	209.0378	0.7272	**0.35**	**4.64E-08**	**33.2248**	**0.52**
Pb	**24^{0}C** **35^{0}C** **50^{0}C**	-0.5797 -0.8904 -1.314	7.8079	0.0282	**0.93**	**0.000214**	**17.892**	**0.98**
Zn	**24^{0}C** **35^{0}C** **50^{0}C**	-3.5314 -2.3845 -0.8206	-34.4971	-0.1043	**0.51**	**1.61E-07**	**34.497**	**0.51**
Al	**24^{0}C** **35^{0}C** **50^{0}C**	4.9359 3.1515 0.7183	53.1136	0.1622	**0.996**	**8.55E-08**	**38.013**	**0.999**
As	**24^{0}C** **35^{0}C** **50^{0}C**	1.1957 0.3459 -0.8129	24.1404	0.0773	**0.801**	**0.00554**	**11.5596**	**0.71962**

Table 5b- Thrmodynamic parameters for adsorption of the metal ions (petroleum Factory.

Ions	T ^{0}C	ΔG^0	ΔH^0	ΔS^0	R^2	S*	Ea	R^2
Cr	**24^{0}C** **35^{0}C** **50^{0}C**	8.5149 8.1411 7.6315	18.6054	0.034	**0.45**	**0.069983**	**5.891**	**0.39**
Fe	**24^{0}C** **35^{0}C** **50^{0}C**	-16.93 -17.88 -19.16	8.5092	0.0857	**0.93**	**0.026303**	**5.907**	**0.93**
Mo	**24^{0}C** **35^{0}C** **50^{0}C**	-1.5251 -2.6959 -4.2925	30.0869	0.1064	**0.82**	**2.47E-06**	**27.018**	**0.95**
Sb	**24^{0}C** **35^{0}C** **50^{0}C**	-7.2747 -7.9217 -8.8039	10.1934	0.0588	**0.84**	**0.008579**	**10.148**	**0.84**
Se	**24^{0}C** **35^{0}C** **50^{0}C**	6.6459 2.7639 -2.5299	111.4618	0.3529	**1.00**	**1.11E-14**	**77.832**	**0.98**
V	**24^{0}C** **35^{0}C** **50^{0}C**	6.7379 6.1593 5.3703	22.3612	0.0526	**0.98**	**0.008332**	**10.576**	**0.95**

REFERENCES

[1] Borszeki, G. Knapp, P.Halmos, L. Bartha;Microchimica Acta 108 (1992) 157-161.

[2] Zhiyong Z., Delong K., Huiying Z., Nian W., Zhongqi R.; Journal of Hazardous Materials 341 (2018) 355-364.

[3] Shaobing G., Wangchang G., Xiaowei H., Jiawei Z., Qiuyu Z.; Colloids and Surfaces A: Physicochemical and Engineering Aspects 539 (2018) 154-162.

[4] Kexin Z., Haiyan L., Xingjian X., Hongwen Y.; Microporous and Mesoporous Materials 255 (2018) 7-14.

[5] Jérémie C., Corina B., Nadia M., Bertrand S., Grégorio C.; Journal of Saudi Chemical Society 20 (2016) 185-194..

[6] Mary M.B., Umadevi M., Pandiarajan S., Ramakrishnan V.; Spectrochimica Acta Part A: Molecular and Biomolecular Spectroscopy 60 (2004) 2643-2651.

[7] Schiewer S., Balaria A.; Chemical Engineering Journal 146 (2009) 211-219.

[8] Ahmad R., Kumar R., Haseeb S.; Arabian Journal of Chemistry 5 (2012) 353-359.

[9] Jian Z., Wenkun Z., Jie Y., Hongping Z., Xuegang L.; Applied Surface Science 435 (2018) 920-927.

[10] Daniela S. S., Irina M.;Comptes Rendus Chimie 17 (2014) 496–502.

[11] Stafiej A., Pyrzynska K.; Separation and Purification Technology 58 (2007) 49-52.

[12] Li Y., Ding J., Luan Z., Di Z., Zhu Y., Xu C., Wu D., Wei B.; Carbon, 41 (2003) 2787-2792.

[13] Atanassova I.; **Environmental Pollution** 87 (1995) 17-21.

[14] Gao Z., Bandosz T., Zhao Z., Han M., Qiu J.; Journal of Hazardous Materials. 167 (2009) 357-365.

[15] Srivastava P., Singh B., Angove M.; Journal of Colloid and Interface Science., 290 (2005) 28-38.

[16] Lagergren S.; Kungliga S. Vetenskapsakademiens, Handlingar 24 (1898) 1-39.

[17] Ho Y.S., G. McKay; Water Research 34 (2000) 735-742.

[18] Nahid Ghasemi, Maryam Ghasemi, Saleh Moazeni, Parisa Ghasemi, Alexey G. Tkachev; Journal of Industrial and Engineering Chemistry, In press (2018).

[19] Weber W.J., J.C. Morris; Journal of the Sanitary Engineering Division - American Society of Civil Engineers 89 (1963) 31-60.

[20] Jiseon J., Dae S. L.; Science of the Total Environment 615 (2018) 549–557.

[21] Naushad M., ALOthman Z.A., Inamuddin, Javadian H.; Journal of Industrial and Engineering Chemistry 25 (2015) 35–41.

[22] Anna W., Zbigniew H.; Microporous and Mesoporous Materials 224 (2016) 400-414.

[23] Singh, B., Das, S.K., Colloids and Surfaces B: Biointerfaces 107 (2013) 97– 106.

[24] Anirudhan T.S., P.G. Radhakrishnan; The Journal of Chemical Thermodynamics 40 (2008) 702–709.